J|A|C|S
ARTICLES
Published on Web 03/28/2007

Mechanistic Insight into Hydrosilylation Reactions Catalyzed by High Valent Re≡X (X = O, NAr, or N) Complexes: The Silane (Si−H) Does Not Add across the Metal−Ligand Multiple Bond

Guodong Du, Phillip E. Fanwick, and Mahdi M. Abu-Omar*

Contribution from the Brown Laboratory, Department of Chemistry, Purdue University, 560 Oval Drive, West Lafayette, Indiana 47907

Received December 12, 2006; E-mail: mabuomar@purdue.edu

Abstract: Treatment of oxo and imido-rhenium(V) complexes $Re(X)Cl_3(PR_3)_2$ (X = O, NAr, and R = Ph or Cy) (**1**−**2**) with Et_3SiH affords $Re(X)Cl_2(H)(PR_3)_2$ in high yields. Cycloaddition of silane across the Re≡X multiple bonds is not observed. Two rhenium(V) hydrides (X = O and R = Ph, **4a**; X = NMes and R = Ph, **5a**) have been structurally characterized by X-ray diffraction. The kinetics of the reaction of $Re(O)Cl_3(PPh_3)_2$ (**1a**) with Et_3SiH is characterized by phosphine inhibition and saturation in [Et_3SiH]. Hence, formation of $Re(O)Cl_2(H)(PPh_3)_2$ (**4a**) proceeds via a σ-adduct followed by heterolytic cleavage of the Si−H bond and transfer of silylium (Et_3Si^+) to chloride. Oxo and imido complexes of rhenium(V) (**1**−**2**) as well as their nitrido analogues, $Re(N)Cl_2(PR_3)_2$ (**3**), catalyze the hydrosilylation of PhCHO under ambient conditions, with the reactivity order imido > oxo > nitrido. The isolable oxorhenium(V) hydride **4a** reacts with PhCHO to afford the alkoxide $Re(O)Cl_2(OCH_2Ph)(PPh_3)_2$ (**6a**) with kinetic dependencies that are consistent with aldehyde coordination followed by aldehyde insertion into the Re−H bond. The latter (**6a**) regenerates the rhenium hydride upon reaction with Et_3SiH. These stoichiometric reactions furnish a possible catalytic cycle. However, quantitative kinetic analysis of the individual stoichiometric steps and their comparison to steady-state kinetics of the catalytic reaction reveal that the observed intermediates do not account for the predominant catalytic pathway. Furthermore, for $Re(O)Cl_2(H)(PCy_3)_2$ and $Re(NMes)Cl_2(H)(PPh_3)_2$ aldehyde insertion into the Re−H bond is not observed. Therefore, based on the kinetic dependencies under catalytic conditions, a consensus catalytic pathway is put forth in which silane is activated via σ-adduct formation *cis* to the Re≡X bond followed by heterolytic cleavage at the electrophilic rhenium center. The findings presented here demonstrate the so-called Halpern axiom, the observation of "likely" intermediates in a catalytic cycle, generally, signals a nonproductive pathway.

Introduction

Catalytic hydrosilylation is an attractive method for the reduction of ketones and aldehydes because it affords silyl protected alcohols in one step under mild conditions.[1] Definitive mechanistic determinations of the process are rare,[2] partly due to the complicated behavior and kinetic dependencies of these reactions. Consequently, mechanistic generalizations are cautioned.[3] Nevertheless, the most widely accepted mechanism, proposed by Chalk and Harrod[4] for alkene hydrosilylation and later adopted by Ojima et al.[5] for carbonyl substrates, adheres to the following sequence: oxidative addition of Si−H, insertion of substrate into a metal hydride (M−H) bond, and reductive elimination of the product. Recently high-valent transition metal oxo complexes of $Re^{V,VII}$ and Mo^{VI} have been utilized in catalytic hydrosilylation reactions.[6−9] In one example, namely *cis*-$Re(O)_2I(PPh_3)_2$, Toste et al. proposed an unconventional mechanism in which the silane (Si−H) adds across one of the

(1) For recent reviews, see: (a) Ojima, I.; Li, Z.; Zhu, J. In *The Chemistry of Organic Silicon Compounds*; Rappoport, Z., Apeloig, Y., Eds.; John Wiley & Sons: New York, 1998. (b) Nishiyama, H.; Itoh, K. In *Catalytic Asmmetric Synthesis*; Ojima, I., Ed.; Wiley-VCH: New York, 2000; Chapter 2. (c) Carpentier, J. -F.; Bette, V. *Curr. Org. Chem.* **2002**, *6*, 913−936. (d) Riant, O.; Mostefai, N.; Courmarcel, J. *Synthesis* **2004**, *18*, 2943−2958.

(2) (a) Reyes, C.; Prock, A.; Giering, W. P. *Organometallics* **2002**, *21*, 546−554. (b) Parks, D. J.; Blackwell, J. M.; Piers, W. E. *J. Org. Chem.* **2000**, *65*, 3090−3098. (c) Zheng, G. Z.; Chan, T. H. *Organometallics*, **1995**, *14*, 70−79. (d) Waldman, T. E.; Schaefer, G.; Riley, D. P. *ACS Symp. Ser.* **1993**, *No. 517*, 58. (e) Kolb, I.; Hetflejs, J. *Collect. Czech. Chem. Commun.* **1980**, *45*, 2224.

(3) Collman, J. P.; Hegedus, L. S.; Norton, J. R.; Finke, R. G. *Principles and Application of Organotransition Metal Chemistry*; University Science Books: Mill Valley, California, 1987; p 564.

(4) Chalk, A. J.; Harrod, J. F. *J. Am. Chem. Soc.* **1965**, *87*, 16.

(5) Ojima, I.; Kogure, T.; Kumagai, M.; Horiuchi, S.; Sato, Y. *J. Organomet. Chem.* **1976**, *122*, 83.

(6) Kennedy-Smith, J. J.; Nolin, K. A.; Gunterman, H. P.; Toste, F. D. *J. Am. Chem. Soc.* **2003**, *125*, 4056−4057.

(7) (a) Ison, E. A.; Trivedi, E. R.; Corbin, R. A.; Abu-Omar, M. M. *J. Am. Chem. Soc.* **2005**, *127*, 15374−5. (b) Ison, E. A.; Cessarich, J. E.; Du, G.; Fanwick, P. E.; Abu-Omar, M. M. *Inorg. Chem.* **2006**, *45*, 2385−2387. (c) Du, G.; Abu-Omar, M. M. *Organometallics* **2006**, *25*, 4920−3. (d) Ison, E. A.; Corbin, R. A.; Abu-Omar, M. M. *J. Am. Chem. Soc.* **2005**, *127*, 11938−9.

(8) (a) Royo, B.; Romao, C. C. *J. Mol. Catal. A: Chem.* **2005**, *236*, 107−112. (b) Fernandes, A. C.; Fernandes, R.; Romao, C. C.; Royo, B. *Chem. Commun.* **2005**, 213−4. (c) Reis, P. M.; Romao, C. C.; Royo, B. *Dalton Trans.* **2006**, 1842−1846.

(9) For reduction of imines and other substrates, see: (a) Nolin, K. A.; Ahn, R. W.; Toste, F. D. *J. Am. Chem. Soc.* **2005**, *127*, 12462−3. (b) Fernandes, A. C.; Romao, C. C. *Tetrahedron Lett.* **2005**, *46*, 8881−8883. (c) Fernandes, A. C.; Romao, C. C. *Tetrahedron* **2006**, *62*, 9650−4. (d) Fernandes, A. C.; Romao, C. C. *J. Mol. Catal. A: Chem.* **2006**, *253*, 96−98.

10.1021/ja068872+ CCC: $37.00

Scheme 1. Postulated Reaction Pathways for Silane Activation with Electrophilic Oxorhenium(V) Complexes

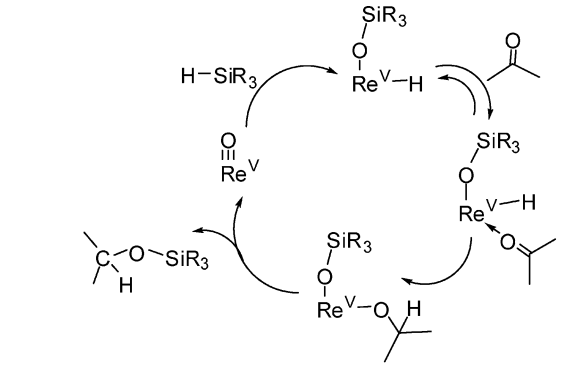

Activation of silane at rhenium oxo bond

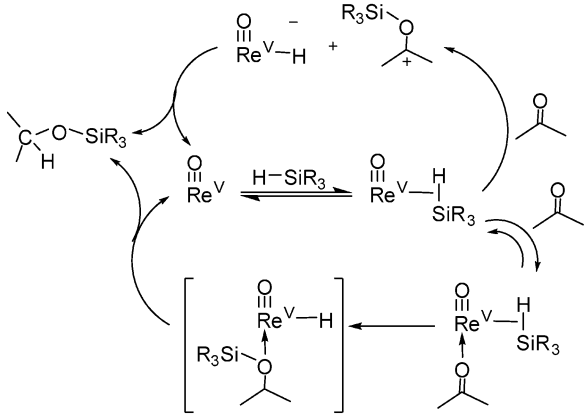

Activation of silane via σ-bond complex

Re≡O multiple bonds.[6] On the other hand, we have shown that cationic monooxo rhenium(V) complexes containing oxazoline and salen ancillary ligands do not utilize the Re≡O bond in catalysis.[7] Our kinetic and mechanistic analysis of monooxo rhenium complexes is consistent with formation of an η^2-silane adduct, which parallels some of the steps in the mechanism proposed for catalytic alcoholysis of silanes.[10]

Therefore, the role of the terminal oxo bond in hydrosilylation remains uncertain (Scheme 1). Is it functioning as a Lewis base to activate the Si−H bond? Can high-valent complexes containing multiply bonded ligands other than oxo effect catalysis?[11] To this end, we have investigated a series of rhenium(V) complexes containing different multiply bonded ligands (Re≡X, where X = O, NAr, or N), Chart 1. If the multiple bonds participate in silane activation, these complexes would exhibit vastly different reactivities. $Re(O)Cl_3(PPh_3)_2$ (**1a**) has been shown to catalyze hydrosilylation of organic carbonyl compounds.[8a] The activity of the catalysts in Chart 1 is considerably lower than that of cationic monooxorhenium(V) oxazoline and salen complexes[7] but quite comparable to that of *cis*-$Re(O)_2I(PPh_3)_2$.[6] Under catalytic conditions, we have observed by ^{31}P NMR two major intermediates, $Re(O)Cl_2(H)(PPh_3)_2$ (**4a**) and $Re(O)Cl_2(OCH_2Ph)(PPh_3)_2$ (**6a**). Subsequently we prepared and characterized both complexes **4a** and **6a**. With these compounds in hand, we were able to perform a detailed kinetic study on each individual step of a postulated catalytic cycle. Herein we report our findings on $Re(O)Cl_3(PPh_3)_2$ and related systems (Chart 1), demonstrate that the multiply bonded ligand is not involved in silane activation, and illustrate how detectable/isolable intermediates do not account for the major catalytic pathway. Furthermore, to the best of our knowledge, the reported rhenium imido complexes represent the first examples of hydrosilylation catalysts containing a terminal imido group, although they have been envisioned previously.[11]

Chart 1. Rhenium Complexes Containing Re≡X Multiple Bonds (Where, X = O, NAr, or N) Used in This Study[a]

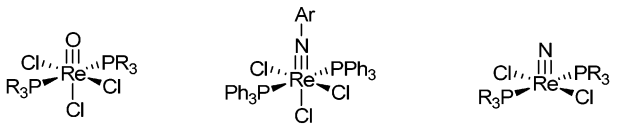

R = Ph (**1a**), Cy (**1b**) Ar = Mes (**2a**), Ph (**2b**) R = Ph (**3a**), Cy (**3b**)

[a] Ph = phenyl, Cy = cyclohexyl, Mes = 2,4,6-trimethyl phenyl.

Results and Discussion

Synthesis and Structure of Oxo and Imido Re^V Hydrides. Treatment of $Re(O)Cl_3(PPh_3)_2$ (**1a**) with excess silane (Et_3SiH) in CH_2Cl_2 resulted in the formation of $Re(O)Cl_2(H)(PPh_3)_2$ (**4a**) in 92% yield, accompanied by the dissolution of **1a** and a color change from yellow to grayish green. The ^{31}P spectrum of **4a** shows a singlet at 8.0 ppm. Even though the hydride resonance is not observable in the ^1H spectrum because it overlaps with aromatic protons from the phosphine ligand, the deuteride labeled compound $Re(O)Cl_2(D)(PPh_3)_2$, prepared from Et_3SiD, shows a resonance at 7.4 ppm in the ^2H NMR spectrum. While metal hydride chemical shifts often appear at negative chemical shifts, positive values have been reported for analogous rhenium hydrides.[12] The IR spectrum exhibits a band at 2018 cm^{-1}, consistent with a Re−H bond.[12] Heterolytic cleavage of the Si−H bond by reaction with the chloride ligand (eq 1) indicates that the chloride ligand, presumably the one trans to the oxo, is more reactive as a base than the terminal oxo in this complex.

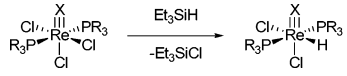

(1)

If the oxo was kinetically more basic in **1a**, migration of silylium to oxo would have afforded rhenium siloxide (Scheme 1). In similar reactions $Re(O)Cl_2(H)(PCy_3)_2$ (**4b**) and $Re(NMes)Cl_2(H)(PPh_3)_2$ (**5a**) were prepared in excellent yields, 79 and 80%, respectively. The rhenium hydrides (Re−H) are observed at 7.70 (**4b**) and 4.74 (**5a**) ppm in the ^1H NMR and at 2034 (**4b**) and 2058 (**5a**) cm^{-1} in the IR. These rhenium hydrides are air and moisture stable and undergo hydride/chloride exchange in CD_2Cl_2 over the course of days to regenerate $Re(X)Cl_3(PR_3)_2$

(10) (a) Luo, X. L.; Crabtree, R. H. *J. Am. Chem. Soc.* **1989**, *111*, 2527−2535. (b) Chang, S.; Scharrer, E.; Brookhart, M. *J. Mol. Catal. A.* **1998**, *130*, 107−119. (c). Matthews, S. L; Pons, V.; Heinekey, D. M. *Inorg. Chem.* **2006**, *45*, 6453−9. (d) Buhl, M.; Mauschick, F. T. *Organometallics* **2003**, *22*, 1422−31.

(11) Thiel, W. R. *Angew Chem.* **2003**, *115*, 5548−5550; *Angew. Chem., Int. Ed.* **2003**, *42*, 5390−5392.

(12) (a) Spaltenstein, E.; Erikson, T. K. G.; Critchlow, S. C.; Mayer, J. M. *J. Am. Chem. Soc.* **1989**, *111*, 617−23. (b) Matano, Y.; Northcut, T. O.; Brugman, J.; Bennet, B. K.; Lovell, S.; Mayer, J. M. *Organometallics* **2000**, *19*, 2781−90. (c) Kim, Y.; Gallucci, J.; Wojcicki, A. *J. Am. Chem. Soc.* **1990**, *112*, 8600−2. (d) Baize, M. W.; Gallucci, J. C.; Wojcicki, A. *Inorg. Chim. Acta* **1997**, *259*, 339−44. (e) Williams, D. S.; Schrock, R. R. *Organometallics* **1993**, *12*, 1148−60.

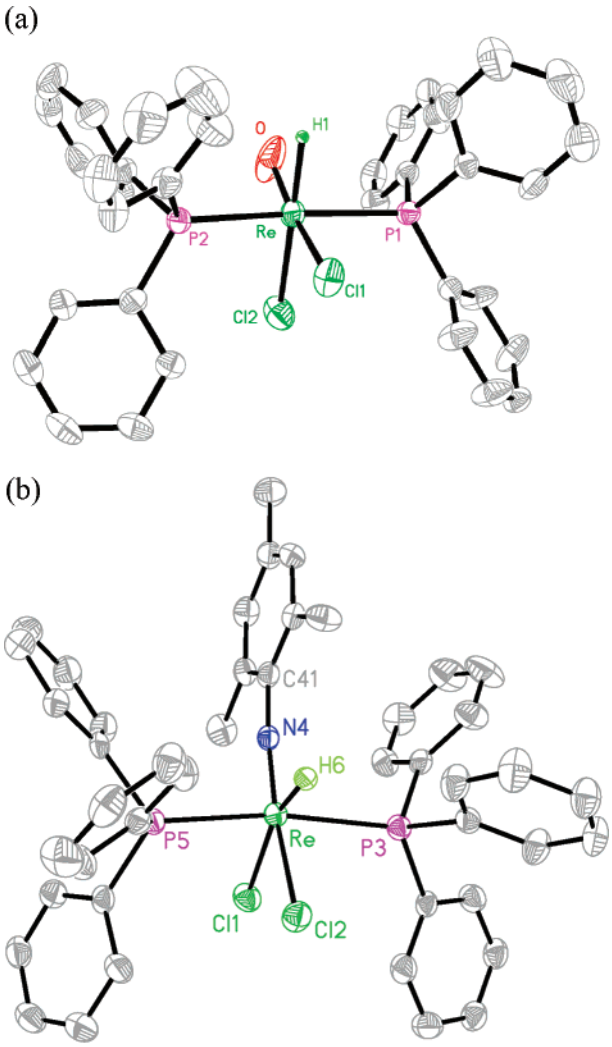

Figure 1. ORTEP diagram (50% probability ellipsoids) of (a) **4a** and (b) **5a**. The hydrogen atoms, except the one on rhenium, are omitted for clarity. Selected bond lengths (Å) and bond angles (deg): (a) Re−O 1.676(6), Re−Cl2 2.4225(17), Re−Cl1 2.4409(16), Re−P2 2.4637(15), Re−P1 2.4741(15), Re−H1 1.73(5), O−Re−Cl1 167.0(3), O−Re−H1 76.5(15); (b) Re−N4 1.719(3), Re−P3 2.4447(11), Re−P5 2.4499(11), Re−Cl2 2.4593(9), Re−Cl1 2.4672(10), Re−H6 1.68(3), N4−C41 1.390(4), N4−Re−Cl2 168.49(10), N4−Re−H6 95.7(10), C41−N4−Re 173.3(3).

(X = O or NAr). Similar degradation in chlorinated solvents has been observed for analogous oxorhenium hydrides.[13]

The molecular structures of **4a** and **5a** were confirmed by single-crystal X-ray diffraction (Figure 1). The structures show a slightly distorted octahedral geometry for rhenium(V) with the hydride ligand *cis* to the multiply bonded oxo or imido group, contrary to earlier speculations that hydride would be trans to the multiply bonded ligand.[14] The phosphine ligands are *trans* with respect to each other and *cis* to the multiply bonded ligands (O or NAr). This stereochemical arrangement leaves the chlorides *cis* to each other. The short bond distance Re−N4 = 1.719(3) Å and the nearly linear C41−N4−Re = 173.3(3)° angle for **5a** are in accord with a Re−N triple bond. The observed stereoisomer in the X-ray structures is in agreement with the solution structure (NMR). The stereoselectivity can be easily rationalized on an electronic basis. The soft ligands

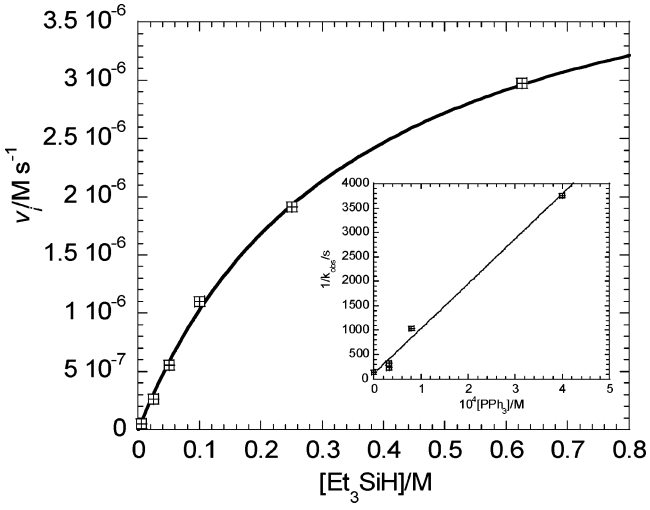

Figure 2. Et_3SiH dependence for its reaction with $ReOCl_3(PPh_3)_2$ (**1a**) to give the rhenium hydride **4a**, monitored by UV−vis spectroscopy. Conditions: 0.20 mM **1a**, CH_2Cl_2, at 25 °C. Inset: $1/k_{obsd}$ versus $[PPh_3]$ for the same reaction. Conditions: 0.20 mM **1a**, 100 mM Et_3SiH, CH_2Cl_2, at 25 °C.

phosphine and hydride occupy sites that are *cis* to the multiply bonded ligand. Hydride is a strong σ-donor, and by adopting a *cis* site to oxo or imido it avoids competition for orbitals with the multiply bonded ligand. On the other hand, PPh_3 maximizes the π interaction between filled d_{xy} on rhenium and σ^* (on PPh_3) by taking up a *cis* site to Re≡X.

Kinetics of Individual Steps. Kinetics of the reaction of **1a** with Et_3SiH, monitored by UV−vis spectroscopy, is somewhat complicated. In the absence of added free PPh_3, the dependence on [**1a**] is not simply first order, as plots of ln[**1a**] versus time are not linear; rather, the kinetic dependence approximates half order.[15] The fractional order dependence is often indicative of a chain reaction mechanism. However, a chain pathway that accounts for the observed product and affords half-order dependence on [**1a**] cannot be envisioned. Furthermore, in the presence of constant [PPh_3] from the onset of the reaction, clean first-order dependence on [**1a**] is observed. Also the analogous reaction with the imido complex **2b** displays first-order dependence on [**2b**] even in the absence of added free PPh_3. Thus, the initial rate method was applied for data analysis for the reaction of **1a** with Et_3SiH in the absence of added PPh_3. The reaction shows saturation behavior with respect to [Et_3SiH] and inhibition by PPh_3 (Figure 2). These dependencies are consistent with substitution of PPh_3 with Et_3SiH followed by Si−H bond cleavage to give the rhenium hydride product. In line with this conclusion, the analogous $ReOCl_3$(dppe) (dppe = 1, 2-bis-(diphenylphosphino) ethane), with a chelating phosphine ligand, does not react with Et_3SiH under similar conditions.

The oxorhenium(V) hydride **4a** undergoes insertion with PhCHO and MeCHO to form the alkoxide complexes $ReOCl_2(OCH_2Ph)(PPh_3)_2$ (**6a**) and $ReOCl_2(OEt)(PPh_3)_2$ (**6b**), respectively,[16] along with a small amount of the corresponding alcohol ($PhCH_2OH$ or EtOH) as a minor byproduct. The kinetics, monitored by ^1H NMR, shows first-order dependence on

(13) Matano, Y.; Brown, S. N.; Northcut, T. O.; Mayer, J. M. *Organometallics* **1998**, 17, 2939−2941.
(14) La Monica, G.; Cenini, S.; Porta, F. *Inorg. Chim. Acta* **1981**, *48*, 91−95.
(15) See Supporting Information for details.
(16) (a) Holder, G. N.; Monteith, G. A. *Transition Met. Chem.* **1992**, *17*, 109−114. (b) Chatt, J.; Rowe, G. A. *J. Chem. Soc.* **1962**, 4019−4033. (c) Graziani, R.; Caselatto, U.; Rossi, R.; Marchi, A. *J. Crystallogr. Spectrosc. Res.* **1985**, *15*, 573−9.

Scheme 2. Mechanism for Reaction of PhCHO with the Hydride **4a**

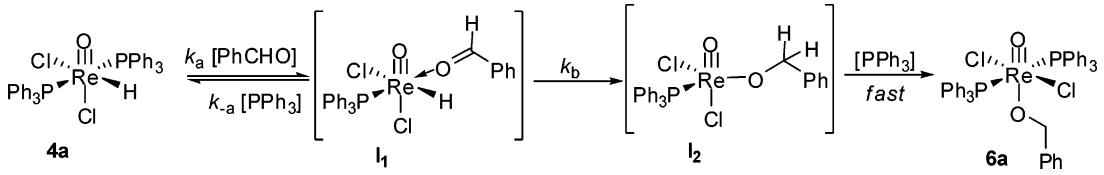

Scheme 3. Mechanism for Reaction of Et_3SiH with the Alkoxide **6a**

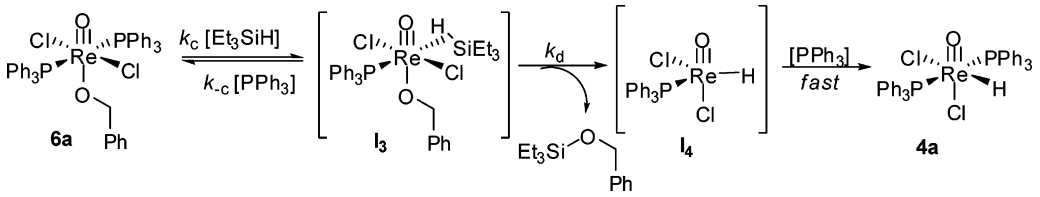

[PhCHO] and [**4a**] in the concentration range investigated, with a second-order rate constant $k_2 = (3.5 \pm 0.3) \times 10^{-3}$ L mol^{-1} s^{-1}. The KIE with $ReOCl_2(D)(PPh_3)_2$ is negligible ($k_2^H/k_2^D = 1.1$). Notably the insertion reactions were also inhibited by PPh_3, demonstrating coordination of the aldehyde (PhCHO or MeCHO) precedes insertion. A kinetic scheme consistent with these observations is depicted in Scheme 2. Assuming the last step is fast, the rate law (steady-state approximation) is given in eq 2. A nonlinear least-squares fit (Figure S-6) gives $k_a = (3.67 \pm 0.05) \times 10^{-3}$ L mol^{-1} s^{-1} and $k_{-a}/k_b = (2.01 \pm 0.01) \times 10^2$ L mol^{-1}. It should be noted that **4b** and **5a** do not undergo insertion with PhCHO or MeCHO under the same conditions; instead, only small amounts of alcohol ($PhCH_2OH$ or EtOH) were detected after a prolonged period of time.

$$\frac{d[\mathbf{6a}]/dt}{[\mathbf{4a}]} = k_{obsd} = \frac{k_a k_b [PhCHO]}{k_{-a}[PPh_3] + k_b} \qquad (2)$$

Treatment of **6a** with Et_3SiH regenerates the hydride **4a**. The kinetics displays first-order dependences on [Et_3SiH] and [**6a**], with a second-order rate constant $k_3 = (9.1 \pm 0.9) \times 10^{-4}$ L mol^{-1} s^{-1}. No kinetic isotope effect was observed with Et_3SiD ($k_3^H/k_3^D = 1.1$). Again, the reaction of **6a** with Et_3SiH was inhibited by PPh_3, suggesting an open coordination site for Et_3SiH is required prior to reaction (Scheme 3).

Mechanistic Considerations of Hydrosilylation with Re≡X. We have independently established three reactions for the $ReOCl_3(PPh_3)_2$ (**1a**) system: (1) formation of the rhenium hydride **4a** via chloride abstraction with silane (eq 1), (2) insertion of carbonyl compounds (aldehydes) into the Re—H bond to form the rhenium alkoxide **6a** (Scheme 2), and (3) silyl ether formation from reaction of the alkoxide complex **6a** with silane to regenerate the rhenium hydride **4a** (Scheme 3). All three steps are combined into Scheme 4 in the form of a catalytic cycle. It is tempting to conclude that this reaction scheme represents the actual catalytic cycle because it satisfies all qualitative observations to this point. Indeed, the intermediate hydride (**4a**) and alkoxide (**6a**) can be readily observed by ^{31}P NMR under catalytic conditions. Further kinetic studies were performed with **4a** as the catalyst because of the poor solubility of **1a** and the formation of Re—H (**4a**) is relatively fast ($k_{obs} \cong 0.02$ s^{-1} at the plateau of Et_3SiH, at low concentration of **1a**). The overall reaction shows approximately first-order dependence on PhCHO and Et_3SiH, while detailed analysis is complicated by the changing distribution of Re catalyst between **4a** and **6a**,

Scheme 4. Fully Characterized Reactions for the $Re(O)Cl_3(PPh_3)_2$ Hydrosilylation Catalyst Shown as a Hypothetical Cycle

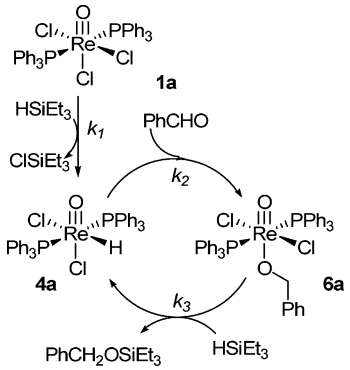

as evidenced by the initial accumulation of **6a** and its subsequent slow disappearance toward the end of the reaction.[15]

Therefore, kinetic simulations were employed to model the catalytic reaction with **4a**, since we have characterized the rate laws for each half of the cycle. However, when the individual steps are put to the test with their respective rate constants into a kinetic simulator, either as a simplified two-step sequence (as in Scheme 4) or as a more detailed six-step sequence (as in Schemes 2 and 3),[15] the resulting steady-state (catalytic) rate of PhCHO consumption is considerably slower than the observed rate for catalytic reaction (Figure 3).[17] Another complicating factor is the very small concentration of free PPh_3 in the reaction. If a minor, unknown, pathway that scavenges free PPh_3 is present under catalytic conditions, it could potentially accelerate the reaction. Therefore, we investigated the reaction kinetics with added PPh_3 (20 mol % relative to **4a**) to buffer the solution and maintain a constant [PPh_3]. While added PPh_3 does slow down the rate of PhCHO consumption, it does not converge with the simulated data (trace d, Figure 3). It is also noteworthy that the experimental PhCHO consumption is almost identical irrespective of the starting form of the rhenium catalyst (**4a** or **6a**) (see traces a and c in Figure 3), despite that each complex enters Scheme 4 with a different rate. These observations suggest that complexes **4a** and **6a** are not the major players in the catalytic pathway, though they are capable of turning over. Based on kinetics, the catalytic pathway presented in Scheme 4 (and detailed mechanisms of each step

(17) The kinetic simulator KINSIM version 4.0 was used with the following rate constants for Scheme 4: $k_2 = 3.5 \times 10^{-3}$ and $k_3 = 9.1 \times 10^{-4}$ M^{-1} s^{-1}. Barshop, B. A.; Wrenn, R. F.; Frieden, C. *Anal. Chem.* **1983**, *130*, 134−145.

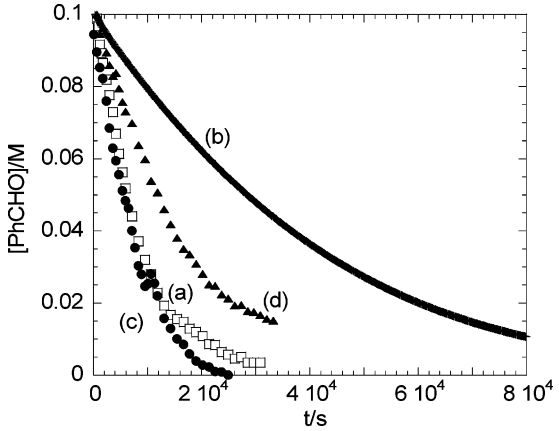

Figure 3. Comparison of experimental PhCHO consumption under catalytic conditions (a, □) and simulations (b, solid line) according to Scheme 4. Conditions: $[ReOCl_2(H)(PPh_3)_2] = 10.0$ mM, [PhCHO] = 101 mM, and $[Et_3SiH] = 664$ mM in CD_2Cl_2 at 25 °C. The program KINSIM along with the experimental values $k_2 = 3.5 \times 10^{-3}$ and $k_3 = 9.1 \times 10^{-4}$ M^{-1} s^{-1} were used to generate the simulated time profile.[15] (c, ●): Using $[ReOCl_2(OCH_2Ph)(PPh_3)_2] = 10.0$ mM as the starting catalyst under the same conditions as those in (a) above. (d, ▲): Same conditions as those in (a) with added PPh_3, 2.0 mM.

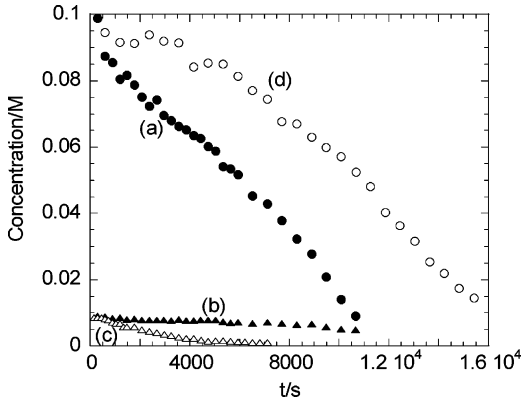

Figure 4. Benzaldehyde (PhCHO) hydrosilylation catalyzed by rhenium imido complexes. (a) Consumption of PhCHO with [**2a**] = 10.0 mM, [PhCHO] = 100 mM, and $[Et_3SiH] = 665$ mM in CD_2Cl_2 at 25 °C. (b) Consumption of **2a** under the same conditions as those in (a). (c) Consumption of **2a** under the same conditions as those in (a) but in the absence of PhCHO. (d) Consumption of PhCHO under the same conditions as those in (a) except using **4a** (10.0 mM) as catalyst.

in Schemes 2 and 3) accounts at most for only 20% of the silylether product. Therefore, there must be another pathway that is faster than going through the observable rhenium hydride and alkoxide intermediates. However, the active catalyst in the dominant pathway is present at a steady-state concentration and does not accumulate at sufficient concentrations to be observed by conventional spectroscopic methods (NMR or UV−vis).

The kinetics of the rhenium imido complex **2a**, albeit more complex, follows in general similar behavior to that seen for the oxo complex **1a**. However, several distinct observations can be made for **2a** as a hydrosilylation catalyst. The imido hydride **5a** is not observed in appreciable concentrations until the end of the catalytic reaction. The generation of **5a** is much faster in the absence of substrate, PhCHO, and reactions starting from **5a** as catalyst are slower than starting with **2a** (Figure 4). More importantly, the rhenium imido hydride **5a** does not undergo aldehyde insertion, which is compelling evidence that the hydride is not an active form of the catalyst in the imido system.

Table 1. Catalytic Hydrosilylation of PhCHO with Et_3SiH[a]

entry	catalyst	time/h	conversion%	yield%[b]
1	$Re(O)Cl_3(PPh_3)_2$ (**1a**)	122	98	88
2	$Re(O)Cl_3(PCy_3)_2$ (**1b**)	100	97	100
3	$Re(O)Cl_2H(PPh_3)_2$ (**4a**)	48	88	83
4	$Re(NPh)Cl_3(PPh_3)_2$ (**2b**)	17	99	100
5	$Re(NMes)Cl_3(PPh_3)_2$ (**2a**)	24	99	100
6	$Re(NMes)Cl_3(PPh_3)(NH_2Mes)$ (**7**)	10	99	100
7	$Re(N)Cl_2(PPh_3)_2$ (**3a**)	103	29	79
8	$Re(N)Cl_2(PCy_3)_2$ (**3b**)	114	18	89

[a] Reaction conditions: 0.9 mmol of PhCHO (~1 M) and Re catalyst (1 mol %) in CD_2Cl_2, 1.5 equiv of Et_3SiH added last at ambient temperature. The reaction was followed by ^1H NMR. [b] Refers to the silylether product. The remaining balance for yields lower than 100% is accounted for by the minor product dibenzyl ether.

Comparison of Re≡X Catalysts. We also compared the reactivities of the catalysts in Chart 1 and a related imido complex *mer*,*trans*-$Re(NMes)Cl_3(PPh_3)(NH_2Mes)$ (**7**) toward hydrosilylation of PhCHO with Et_3SiH in an effort to gain insight regarding the role of the terminal multiple bond in catalysis. On a preparative scale (~1 mmol PhCHO), all of these complexes are active with varying efficiency (Table 1 and Figure S-11). One caveat here is the complexes' poor solubility in common organic solvents, and the relatively high concentration of nonpolar silane (~1.5 M) employed under catalytic conditions further limits their solubility. Surprisingly introduction of the more lipophilic phosphine, PCy_3, does not improve matters much. Hence, the comparison of catalytic activity made under preparative conditions is qualitative. Nevertheless, it is significant that the rhenium imido catalysts are more reactive than their oxo analogues. Additionally increasing steric bulk as in the mesityl imido ligands (entries 5 and 6) has little effect on reactivity. Replacement of one PPh_3 ligand with an amine ligand in **7** enhances the catalytic activity, presumably because the amine ligand is more labile than PPh_3. Despite being five-coordinate, the rhenium nitride catalysts exhibit the lowest activity of the series. This observation is consistent with the strong trans influence of the nitrido ligand and sluggish substitution rates in $Re(N)Cl_2(PR_3)$.

The oxo and imido complexes investigated in this study (entries 1−6) are 2 orders of magnitude less reactive than cationic monooxo salen and oxazoline complexes of rhenium(V).[7a−c] The latter catalysts require only 0.1 mol % catalyst loading and a reaction time of a few hours under ambient conditions. However, catalysts **1**, **2**, and **7** are comparable or slightly more reactive than *cis*-$Re(O)_2I(PPh_3)_2$.[6]

What Is the Hydrosilylation Mechanism for Re≡X Catalysts? We have so far considered two pathways by which silane can be activated by $Re(X)Cl_n(PR_3)_2$: (1) Activation by the Re≡X bond via [2 + 2] cycloaddition across the Re≡X bond (Scheme 1);[6] and (2) Silane−ligand (chloride or alkoxide) metathesis, as shown for the present systems (Scheme 4). The fact that the imido Re complexes are more active than their oxo analogues and are not sensitive to steric bulk (mesityl versus phenylimido) speaks against the direct involvement of the Re≡X bond. Furthermore, the cycloaddition pathway can be ruled out because the kinetics of a $ReOCl_3(PPh_3)_2$−Et_3SiH reaction shows saturation in silane and inhibition by PPh_3. Also the metathesis reaction affords a Re^V hydride that is not sufficiently reactive to account for the observed catalytic turnover. Moreover, kinetic analysis of the rhenium imido

Scheme 5. Proposed Mechanism(s) for Activation of Silane via Heterolytic Cleavage with Re≡X Catalysts

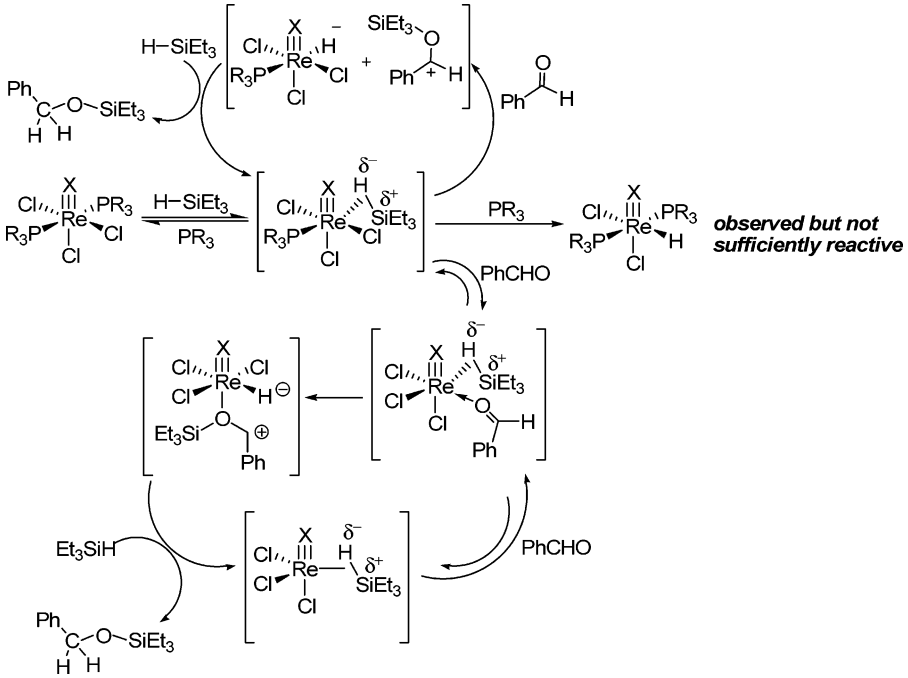

catalyst refutes the participation of the rhenium hydride **5a**, as well as the involvement of the multiply bonded ligand on rhenium.

Two possibilities, hence, remain: oxidative addition of silane to Re^V or heterolytic cleavage via a σ-bond η^2-silane adduct. Although neither intermediate can be observed, we prefer the latter on the grounds that, by analogy to dihydrogen activation,[18] oxidative addition proceeds by homolytic cleavage of the Si−H bond, which is unlikely for electrophilic metals like Re^V. The rate-determining steps would be substitution of the phosphine ligand by silane, which is in agreement with the kinetic dependencies and small KIE values observed throughout. By coordinating *cis* to the Re^V≡X multiple bond, the silane lies in plane with the filled d_{xy} orbital on rhenium maximizing π-back-donation from d_{xy} into σ^* of the Si−H bond. This would, at least in part, explain the low activity of nitrido rhenium complexes (Table 1). Activation of silanes by rhenium nitride (Re≡N) complexes would require isomerization to trigonal bipyramidal geometry or PPh_3 dissociation to form a four-coordinate species; both would be high-energy species. The rhenium−silane σ-adduct affords Si−H heterolytic cleavage in one of three ways: (1) Silylium (Et_3Si^+) transfers to chloride (or alkoxide) to give Re^V hydride, which either accounts for a minor fraction of the catalysis (as in **1a**) or is inactive toward aldehyde (as in **1b** and **2a**). (2) Silylium (Et_3Si^+) transfers to the substrate (PhCHO) followed by recombination of the activated aldehyde and rhenium hydride. This pathway resembles the catalytic ionic hydrogenation mechanism advanced by Bullock in which metal hydrides act as H^- donors to activated carbonyl compounds.[19] Alternatively, aldehyde reduction could proceed in a more concerted fashion; i.e., the bound, electrophilic silicon in the silane complex is attacked by the aldehyde oxygen followed by the transfer of H^-. Theoretical studies have indicated that nucleophilic attack of alcohol on bound silicon is energetically favorable in catalytic silane alcoholysis.[10d] (3) Aldehyde (PhCHO) coordinates in place of another ligand (most likely phosphine), and Et_3Si^+ transfers to the aldehyde ligand to give an activated silylether at the metal, which combines intramolecularly with the hydride ligand. This pathway is less plausible because it requires substitution of both phosphine ligands with two weakly bound ligands. These pathways are summarized in Scheme 5.

In light of our results reported herein, a comment on the hydrosilylation catalyst *cis*-$Re(O)_2I(PPh_3)_2$ is in order.[6] The postulated mechanism for *cis*-$Re(O)_2I(PPh_3)_2$ is likely to be the exception rather than the rule for hydrosilylation reactions catalyzed by high-valent oxorhenium complexes. Notwithstanding the lack of quantitative scrutiny, if indeed silane (Si−H) addition to the Re≡O bond turns out to be catalytically relevant to the dioxorhenium(V) system, this contrast to the general monooxo complexes investigated herein can be attributed to the uniqueness of *cis*-$Re(O)_2I(PPh_3)_2$ in that it features an unconventional *cis* dioxo core (instead of the expected *trans* for a d^2 configuration) and is five-coordinate.[20] A recent *in silico* investigation of hydrosilylation supports silane addition to the Re≡O bond in *cis*-$Re(O)_2I(PR_3)_2$, interestingly via a dissociative [2 + 2] pathway in which silane replaces a phosphine ligand on rhenium.[21] The same study concludes that the second oxo promotes the [2 + 2] addition (kinetically and thermodynamically) in comparison to the neutral monooxo complex Re(O)-$Cl_3(PMe_3)_2$. Despite computational results, we show in this report experimentally that neutral monooxo complexes of the type $Re(O)Cl_3(PR_3)_2$ do not undergo silane addition across the Re≡O bond.

Concluding Remarks. It is often understood but not explicitly stated that definitive conclusions of mechanistic studies are

(18) (a) Kubas, G. J. *Metal-Dihydrogen and σ-Bond Complexes: Structure, Bonding, and Reactivity*; Kluwer Academic/Plenum: New York, 2001. (b) Kubas, G. J. *Adv. Inorg. Chem.* **2004**, *56*, 127. (c) Morris, R. H. *Can. J. Chem.* **1996**, *74*, 1907. (d) Kubas, G. J. *Science* **2006**, *314*, 1096.

(19) (a) Bullock, R. M. *Chem.—Eur. J.* **2004**, *10*, 2366. (b) Bullock, R. M.; Voges, M. H. *J. Am. Chem. Soc.* **2000**, *122*, 12594.

(20) Lin, Z.; Hall, M. B. *Coord. Chem. Rev.* **1993**, *123*, 149−167.

(21) Chung, L. W.; Lee, H. G.; Lin, Z.; Wu, Y.-D. *J. Org. Chem.* **2006**, *71*, 6000−6009.

a refutation of possible mechanisms rather than proof of a given reaction mechanism. By this scientific standard results from this study have shown decisively that the terminal multiple bonds Re≡X (X = O, NAr, or N) in $Re(X)Cl_n(PR_3)_2$ (where $n = 2$ or 3) hydrosilylation catalysts neither are directly involved in silane activation nor undergo [2 + 2] cycloaddition with silane (Si−H). Furthermore, we show that the observable and isolable intermediates are not the major players in the catalytic pathway. This underscores the importance of obtaining quantitative kinetic information in elucidating reaction mechanisms, particularly those of catalytic reactions because frequently what is seen is not what is responsible for catalysis, even in cases when stoichiometric reactivity for each of the intermediates could be independently established.[22,23] By process of elimination, complexation of η^2-silane *cis* to the Re≡X bond followed by heterolytic cleavage is the most viable catalytic pathway for the series $Re(X)Cl_n(PR_3)_2$ (X = O, NAr, or N; $n = 2$ or 3; and R = Ph or Cy).

Experimental Section

Materials and Instruments. All manipulations were performed under air unless stated otherwise. Solvents were purified with a solvent purification system (Anhydrous Engineering Inc.) prior to use. Organosilanes and carbonyl compounds were obtained from commercial sources and used as received. NMR spectra were recorded on a Varian Inova 300 or Mercury 200 instrument at 20 °C. Proton resonances were referenced internally to residual solvent peaks ($CHDCl_2$, δ 5.32). Infrared spectra were recorded as KBr pellets on a Perkin-Elmer 2000 FT−IR spectrometer. UV−vis data were recorded on a Shimadzu 2501 spectrophotometer and reported as λ_{max} in nm (log ϵ). Mass spectrometry was performed by the Purdue University Campus Wide Mass Spectrometry Center using a Hewlett-Packard Engine mass spectrometer (GC/MS). Elemental microanalyses were done by the Purdue University Microanalytical Laboratory. Kinetic runs were carried out on a Shimadzu 2501 spectrophotometer or a Varian Inova 300 NMR instrument at 25 °C. Data analyses were performed using KaleidaGraph, version 3.6.

$Re(O)Cl_2(H)(PPh_3)_2$ (4a). To a yellow suspension of $ReOCl_3(PPh_3)_2$ (203 mg, 0.244 mmol) in CH_2Cl_2 (10 mL) was added Et_3SiH (200 μL, 1.25 mmol). After being stirred at ambient temperature for 4.5 h, the mixture was filtered and the yellow-green filtrate was dried under vacuum. The resulting material was washed with pentane to give **4a**. Yield: 180 mg (92%). X-ray quality crystals were grown by gas-phase diffusion of pentane into a CH_2Cl_2 solution in the presence of a small amount of Et_3SiH. ^{1}H NMR (CD_2Cl_2, 300 MHz): δ 7.78 (m, 12H), 7.47 (m, 19H, aromatic C*H* and Re*H*). ^{31}P NMR (CD_2Cl_2, 121.4 MHz): δ 8.0 ppm (s). FT−IR (KBr): 2018 (Re−H), 990 (Re≡O) cm^{-1}. Anal. Calcd (found) for $C_{36}H_{31}Cl_2OP_2Re$: C, 54.14 (54.50); H, 3.91 (4.03). $Re(O)Cl_2(D)(PPh_3)_2$ was prepared similarly from $ReOCl_3(PPh_3)_2$ and Et_3SiD (Aldrich, 97 atom % D).

$ReOCl_2(H)(PCy_3)_2$ (4b). To a yellow suspension of $ReOCl_3(PCy_3)_2$ (180 mg, 0.207 mmol) in CH_2Cl_2 (10 mL) was added Et_3SiH (190 μL, 1.19 mmol). After being stirred at ambient temperature for 5.5 h, the mixture was filtered and the yellow-green filtrate was dried under vacuum. This resulting material was triturated and washed with pentane to give **4b**. Yield: 137 mg (79%). ^{1}H NMR (CD_2Cl_2, 300 MHz): δ 7.70 (t, J = 16.2 Hz, 1H, Re*H*), 2.8−1.2 (m, 66H, PCy_3). ^{31}P NMR (CD_2Cl_2, 121.4 MHz): δ 10.0 ppm (s). FT−IR (KBr): 2034 (Re−H), 992 (Re≡O) cm^{-1}. Anal. Calcd (found) for $C_{36}H_{67}Cl_2OP_2Re$: C, 51.78 (51.40); H, 8.09 (7.75).

$Re(NMes)Cl_2(H)(PPh_3)_2$ (5a). To a green solution of $Re(NMes)Cl_3(PPh_3)_2$ (155 mg, 0.151 mmol) in CH_2Cl_2 was added Et_3SiH (120 μL, 0.751 mmol). The reaction mixture was stirred at ambient temperature for 18 h in which the color changed from green to yellow to dark red. The solvent was removed under vacuum, and the residue was triturated with pentane. The light brown powder was collected by filtration and washed with pentane. Yield: 110 mg (80%). X-ray quality crystals were grown by gas-phase diffusion of pentane into a benzene solution. ^{1}H NMR (CD_2Cl_2, 300 MHz): δ 7.75 (m, 12H), 7.27 (m, 18H), 6.37 (s, 1H), 6.16 (s, 1H), 4.74 (t, 1H, J = 17.1 Hz, Re*H*), 1.98 (s, 3H), 1.77 (s, 3H), 1.40 (s, 3H). ^{13}C NMR (CD_2Cl_2, 75 MHz): δ 138.3, 137.3, 134.8, 134.2, 133.8, 133.3, 130.3, 129.7, 129.1, 128.1, 22.9, 20.1, 19.7. ^{31}P NMR (CD_2Cl_2, 121.4 MHz): δ 10.1 ppm (s). FT−IR (KBr): 2058 cm^{-1} (Re−H). ESI-MS: 912/914/916 $(M - H)^+$, 878/880 $(M - Cl)^+$ with correct isotopic pattern. Anal. Calcd (found) for $C_{45}H_{42}Cl_2NP_2Re\cdot 1.5C_6H_6$: C, 62.78 (62.60); H, 4.98 (5.04); N, 1.36 (1.35).

$Re(NMes)Cl_3(PPh_3)(NH_2Mes)$ (7). A suspension of $ReOCl_3(PPh_3)_2$ (721 mg, 0.865 mmol) and 2,4,6-trimethylaniline (1 mL, 7.10 mmol) was allowed to reflux for 48 h in dry benzene (35 mL). The resulting dark green solution was stripped off the solvent and treated with a mixture of acetic acid−H_2O (1:1). The green precipitate was collected by filtration and redissolved in hot benzene. After filtration, the filtrate was allowed to stand for several days. The green crystals were collected by filtration. Yield: 361 mg (48%). X-ray quality crystals were grown from a benzene solution of **7**. In the filtrate, $Re(NMes)Cl_3(PPh_3)_2$ could be isolated. ^{1}H NMR (CD_2Cl_2, 300 MHz): δ 7.67 (m, 6H), 7.29 (m, 9H), 7.18 (s, 2H, NH_2), 6.71 (s, 2H), 6.39 (s, 2H), 2.30 (s, 6H), 2.21 (s, 3H), 2.11 (s, 3H), 1.60 (s, 6H). ^{31}P NMR (CD_2Cl_2, 121.4 MHz): δ −17.0 ppm (s). ESI-MS: 823/825 $(M + 1)^+$, 785/787/789 $(M - Cl)^+$ with correct isotopic pattern. Anal. Calcd (found) for $C_{36}H_{39}Cl_3N_2PRe\cdot 0.5C_6H_6$: C, 54.32 (54.41); H, 4.91 (4.71); N, 3.25 (3.17).

Kinetics. The reaction of $ReOCl_3(PPh_3)_2$ (**1a**) with Et_3SiH in CH_2Cl_2 was monitored by UV−vis at 430 nm where $ReOCl_3(PPh_3)_2$ has a shoulder absorbance while $ReOCl_2(H)(PPh_3)_2$ does not. Attempts to monitor this reaction by ^{31}P NMR were unsuccessful. The reaction of $Re(NMes)Cl_3(PPh_3)_2$ with Et_3SiH in CH_2Cl_2 was monitored by UV−vis at 360 nm. Other reactions were monitored by ^{1}H NMR in CD_2Cl_2 in the presence of an internal standard (Ph_3CH). The initial rates of the **1a**−Et_3SiH reaction were obtained from a fifth-order polynomial fit of the concentration−time profile, as in $[\mathbf{1a}]_t = [\mathbf{1a}]_0 - m_1t - m_2t^2 - ...-m_5t^5$, from which $v_i = m_1$. Data analysis was performed by a nonlinear least-squares fitting using KaleidaGraph.

X-ray Data Collection and Structure Solution. A summary of structure determination is provided here and further details can be found in the Supporting Information. Crystallographic data for **4a**: $C_{36}H_{31}Cl_2OP_2Re$, FW = 798.70, 0.38 × 0.35 × 0.28 mm^3 crystal dimension, orthorhombic, space group *Pbca* (# 61), a = 18.0285(3) Å, b = 16.6735(3) Å, c = 21.7549(4) Å, V = 6539.5(2) Å^3, Z = 8, ρ_{calcd} = 1.622 g/cm^3, u = 40.5/cm, 58 558 reflections collected, 8408 unique (R_{int} = 0.067), R1 = 0.055, R2 = 0.146, for 5437 reflections with $F_o^2 > 2\sigma(F_o^2)$. Crystallographic data for **5a**: $C_{45}H_{42}Cl_2NP_2Re$, $1.5(C_6H_6)$, FW = 1033.07, 0.35 × 0.35 × 0.15 mm^3 crystal dimension, monoclinic, space group *P*121/*n*1(# 14), a = 15.3680(3) Å, b = 19.1680(3) Å, c = 15.9227(4) Å, β = 103.2930(7)°, V = 4564.74(16) Å^3, Z = 4, ρ_{calcd} = 1.50 g/cm^3, u = 29.2/cm, 42 473 reflections collected, 11 165 unique (R_{int} = 0.054), R1 = 0.042, R2 = 0.069, for 7192 reflections with $F_o^2 > 2\sigma(F_o^2)$. Crystallographic data for **7**: $C_{36}H_{39}Cl_3N_2PRe$, $0.5(C_6H_6)$, FW = 862.32, 0.27 × 0.20 × 0.11 mm^3 crystal dimension, triclinic, space group P_{-1}(# 2), a = 11.8396(5) Å, b = 12.8071(5) Å, c = 13.6137(7) Å, α = 72.664(2)°, β = 76.118(2)°, γ

(22) (a) Halpern, J. *Science*, **1982**, *217*, 401−7. (b) Chan, A. S. C.; Pluth, J. J.; Halpern, J. *J. Am. Chem. Soc*. **1980**, *102*, 5952−4.

(23) This truism has been referred to as the Halpern axiom or Halpern's rule. For example, see: (a) Darensbourg, D. J.; Darensbourg, M. Y.; Goh, L. Y.; Luvig, M.; Wiegreffe, P. *J. Am. Chem. Soc*. **1987**, *109*, 7539−40. (b) Yin, C.; Xu, Z.; Yang, S.-Y.; Ng, S. M.; Wong, K. Y.; Lin, Z.; Lau, C. P. *Organometallics* **2001**, *20*, 1216−22. (c) Hagen, C. M.; Vieille-Petit, L.; Laurenczy, G.; Suss-Fink, G.; Finke, R. G. *Organometallics* **2005**, *24*, 1819−31. (d) Tschan, M. J. L.; Suss-Fink, G.; Cherioux, F.; Therrein, B. *Chem.—Eur. J.* **2007**, *13*, 292−9.

$= 70.558(2)°$, $V = 1835.28(14)$ Å^3, $Z = 2$, $\rho_{calcd} = 1.56$ g/cm^3, $u = 36.5$/cm, 24 555 reflections collected, 8359 unique ($R_{int} = 0.043$), R1 $= 0.031$, R2 $= 0.057$, for 7054 reflections with $F_o^2 > 2\sigma(F_o^2)$.

Acknowledgment. This research was supported by the Chemical Sciences Division, Office of Basic Energy Sciences, U.S. Department of Energy (Grant No. DE-FG02-06ER15794). We are grateful to Professors William Jones and Elon Ison for valuable discussions.

Supporting Information Available: Full experimental details, kinetic plots, and simulation studies, CIF files giving crystallographic data for **4a**, **5a**, and **7**. This material is available free of charge via the Internet at http://pubs.acs.org.

JA068872+